Hindawi Publishing Corporation
Journal of Nanomaterials
Volume 2014, Article ID 495381, 16 pages
http://dx.doi.org/10.1155/2014/495381

Review Article

Development and Application of Surface Plasmon Polaritons on Optical Amplification

Tong Zhang[1,2] and Feng Shan[1,2]

[1] *School of Electronic Science and Engineering, Southeast University, Key Laboratory of Micro-Inertial Instrument and Advanced Navigation Technology, Ministry of Education, Nanjing, Jiangsu 210096, China*
[2] *Suzhou Key Laboratory of Metal Nano-Optoelectronic Technology, Suzhou Research Institute of Southeast University, Suzhou, Jiangsu 215123, China*

Correspondence should be addressed to Tong Zhang; tzhang@seu.edu.cn

Received 28 February 2014; Accepted 15 May 2014; Published 24 July 2014

Academic Editor: Xuefeng Liu

Propagation of surface plasmon polaritons (SPPs) along the interface between a metal and a dielectric has attracted significant attention due to its unique optical properties, which has inspired a plethora of fascinating applications in photonics and optoelectronics. However, SPPs suffer from large attenuation because of the ohmic losses in the metal layer. It has become the main bottom-neck problem for the development of high performance plasmonic devices. This limitation can be overcome by providing the material adjacent to the metal with optical gain. In this paper, a review of gain compensation to SPPs is presented. We focus on the spontaneous radiation amplification and simulated radiation amplification. The ohmic loss of metal was greatly improved by introducing optical gain. Then we introduce several gain mediums of dye doped, quantum dots, erbium ion, and semiconductor to compensate optical loss of SPPs. Using gain medium mentioned above can compensate losses and achieve many potential applications, for example, laser, amplifier, and LRSPP discussed.

1. Introduction

Surface plasmon polaritons (SPPs) are transverse magnetic (TM) polarized optical surface waves formed through the interaction of photons with free electrons at the surface of metals, typically at visible or infrared wavelengths [1]. This mode has fields that peak at the metal dielectric interfaces, decaying exponentially into the dielectric background. Various metallic structures have been investigated over time [2, 3], leading to potentially interesting applications across many fields including fields such as spectroscopy [4], nanophotonics [5], imaging [6], biosensing [7, 8], and circuitry [9]. In a large part, the rapidly growing interest in SPPs was driven by the eagerness to understand and control the behavior of light on the nanometer scale and enabled by the significant improvements in micro- and nanofabrication that have appeared in the past several decades. The presence of SPPs in metallic nanostructures linked with a variety of distinctive optical performances, such as extraordinary light transmission, huge field enhancement, and negative refraction [4].

Although SPPs waveguides are of the inherent virtue of the subwavelength scale confinement, the propagation length is not long due to the ohmic loss in metals. One of the main limitations in using SPPs for device design is the intrinsic damping of SPPs arising from the loss in the metal. Interband transitions absorption can be reduced by careful selection of the operating wavelength and reducing free electron scattering by improving fabrication techniques; however, it cannot be eliminated completely [10].

SPPs practical applications are limited due to their exceeding loss. Many efforts [11–14] have been made to increase the transmission length and simultaneously assure the subwavelength confinement. Gain compensation approach is proposed by investigator to add optical gain. The compensation of SPPs establishes the foundation for lots of amusing and helpful applications, which has motivated much of the study on it.

The characters of SPPs supported by all kinds of metallic structures are notably different from their traditional counterparts in form and character. Following the introduction, the remainder of this paper is structured as follows: Section 2 will describe two aspects of compensation way, fluorescence enhancement and laser amplification. In Section 3, the gain mediums including dyes, quantum dots (QDs), Er ions, and semiconductors are discussed. A range of emerging applications of gain SPPs are discussed in Section 4. Finally, in Section 5 conclusions are provided.

2. The Ways of SPPs Gain Compensation

As the significance of loss has become more important to the SPPs, a multiaspect effort to mitigate loss has been studied. One can readily classify the variety of approaches to deal with the losses into several categories. The first one is to engineer the shape and size of plasmonic structures with the goal of reducing the fraction of energy confined inside the metal leading to the decrease of the loss. The second one is to choose suitable noble materials such as highly doped semiconductors, intermetallics, and graphene. The third one is to introduce optical gain into the plasmonic structure to compensate the loss. The optical gain, however, not only can compensate the loss, but also can realize amplification. In this section, two kinds of optical amplification mechanisms of SPPs including spontaneous radiation and simulated radiation are discussed.

2.1. Spontaneous Radiation Amplification. In the past decades, many efforts have been devoted to spontaneous radiation-based study [15] with advanced sensitivity by using plasmon enhanced fluorescence [16–18]. In SPPs coupled fluorescence emission, fluorescence emitted by gain medium via SPPs is studied. The outcoupling of fluorescence that is trapped in SPPs to radiation is reported [19–21] to provide efficient means for SPPs signal enhancement.

Sudarkin and Demkovich [22] first reported the SPPs gain compensation of fluorescence enhancement, whose structure contained a silver film sandwiched between a glass prism and a gain medium. Then a similar structure over a wider range of parameters was investigated by Poltz et al. [23]. Recently, increasing efforts have been devoted to the compensation for the SPPs fluorescence enhancement by using gain media to achieve loss compensation [24–30]. Noginov et al. [31] have studied SPPs excited by emission of optically pumped R6G molecules and by direct scattering of pumping light in a polymeric film in the attenuated total reflection setup. As shown in Figure 1, SPPs are confined to the proximity of metal dielectric interface and decay exponentially in both media. In the experiments, increasing the pumping intensity, the character of the SPPs emission excited via optically pumped dye molecules has changed dramatically. The emission spectra considerably narrowed in comparison to those at low pumping.

Besides, SPPs propagation with net positive gain over microscopic distances directs proof by Gather et al. [32]. The schematic illustration of the long range surface plasmon

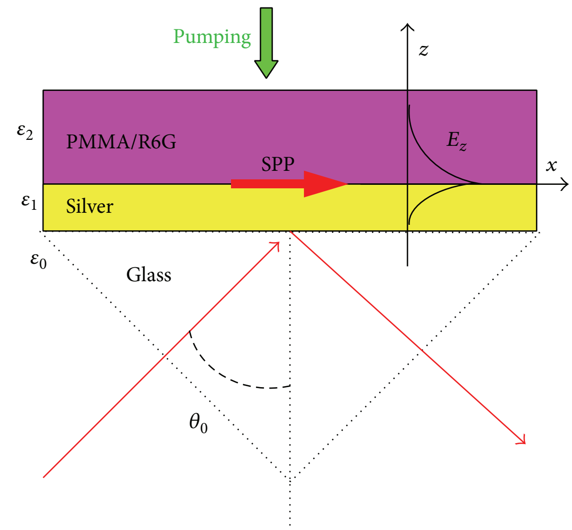

Figure 1: Schematic of experimental sample.

polariton (LRSPP) waveguides is shown in Figure 2(a). The device is composed of a Si substrate layer over a 20 mm thick transparent polymer layer with a refractive index of 1.55 and an Au layer with the thickness of 4 nm. A gain material layer with 1 mm thickness and an additional 20 mm thick transparent polymer layer complete the structure. The end-fire coupled light to the LRSPP mode of waveguides using a low numerical aperture optical fiber to measure the propagation loss of the waveguide at the relevant wavelengths and image the decay of the scattered light intensity along the direction of the light propagation. A waveguide which did not include the gain material layer was measured first. As can be seen from Figure 2(b), the losses at wavelengths higher than 600 nm are below the gain that can be obtained with PPV in this region of the spectrum. However, the propagation loss increases speedily at shorter wavelengths because of the Au surface plasmon resonance. The propagation losses are mostly ascribed to absorption and scattering in the metal film. Propagation loss measurements for waveguides containing a layer of gain material were also discussed in Figure 2(b).

The foregoing researches have discussed SPPs gain on the basis of fluorescence enhancement of gain medium stimulated emission. These works paved the way toward the development of kinds of devices exploiting SPPs amplification. Gain medium excitation provides larger enhancement of the fluorescence excitation and thus allows for a stronger increase in the SPPs signal. Due to the introduction of spontaneous radiation to SPPs, lots of potential applications were developed.

2.2. Simulated Radiation Amplification. Aside from spontaneous radiation amplification, simulated radiation amplification is also used to compensate the SPPs loss, which emerges during the propagation. SPPs are capable of closely localizing light, but up to now ohmic losses at optical frequencies have impeded the realization of nanometer scale lasers [10, 33].

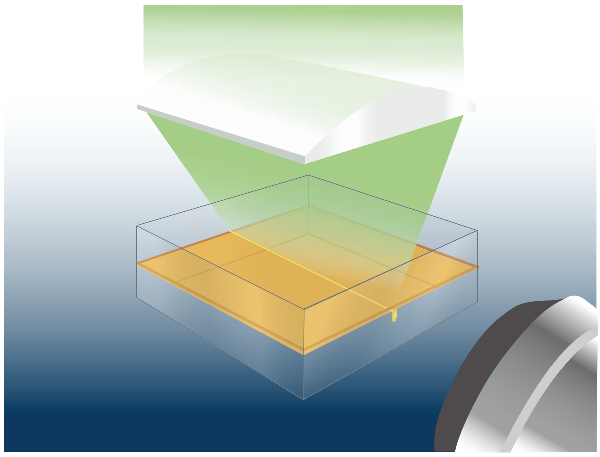

(a)

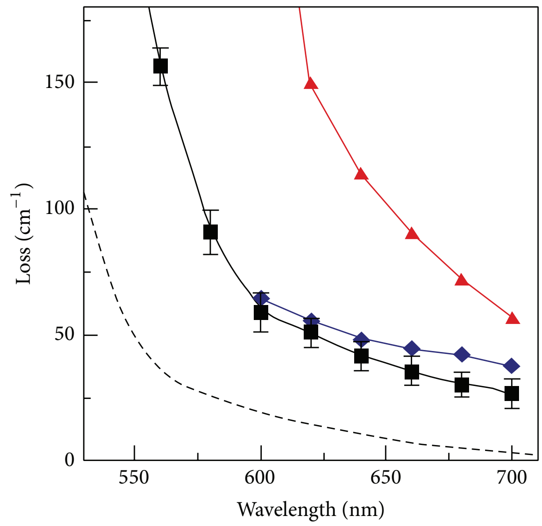

(b)

FIGURE 2: (a) Schematic of LRSPP waveguides containing a fluorescent polymer blend to provide optical gain and illustration of the gain measurement configuration; (b) Measurement and optimization of the propagation loss in 4 nm thick gold LRSPP waveguides. Propagation loss for different plasmonic waveguides as a function of wavelength for a structure without gain material (black squares), with a gain layer that was partly index matched (red triangles, nominal Δn = 0.03) and fully index matched (blue diamonds). Error bars represent uncertainty of the fit to the exponential decay and are representative for all data sets. The dashed line represents a theoretical loss estimate (neglecting scattering) for the structure without gain material.

Through amplifying the radiation by simulated emission, SPPs signal amplification can be achieved. The resonant cavity is used to stimulate more light emission with the same phase by reflecting the light back and forth in metal nanostructures in order to generate the initial SPPs around the nanoscale metal dielectric interface. Oulton et al. [34] first theoretically foretold that such losses could be deeply reduced while maintaining ultrasmall modes in a hybrid plasmonic waveguide. Based on this, Oulton et al. [33] reported the experimental demonstration of nanometer scale plasmonic lasers, generating optical modes a hundred times smaller than the diffraction limit. The coupling between the plasmonic and waveguide modes across the gap enables energy storage in nonmetallic regions. This structure allows SPPs to travel over larger distances with strong mode confinement. Lately, many works focusing on optoelectronic devices and circuits constructed by resonance cavities for SPPs enhancement were studied [35, 36]. One of the cavities for nanowires (NWs) offered great surface smoothness and crystalline structures, which guaranteed low waveguiding losses for plasmonic [37, 38] mode.

The loss compensation ability of the hybrid plasmonic waveguide which is composed of a CdSe nanobelt (NB) kept from a silver surface by an Al_2O_3 layer was investigated experimentally by Liu et al. [39]. An optical pump probe technique was used to probe signals and the ultrahigh optical gain with gain coefficient exceeding 6755 cm^{-1} was achieved. The important thing is that the loss compensation works in the comparatively wide spectral band regime and requires nanolasing operating at single mode. It can be seen from [39] that all wavelengths in the probe signal are equally amplified through the stimulated emission, demonstrating the broadband performance of the loss compensation subject. Internal gain measurements as a function of the pump intensity for probe signals show obvious loss compensation, achieving maximum gain of 8.8 dB.

Wu et al. [40] reported a NWs laser that offers subdiffraction limited beam size and spatially separated plasmon cavity modes. The scheme is illustrated in Figure 3(a). An Ag NW is side coupled to a CdSe NW to form an X-shaped structure (Figure 3(c)). The lasing action is investigated under 532 nm wavelength laser pulses (5 ns pulse width, 2 kHz repetition rate). They mainly focused on the left segment of the CdSe NW (Figure 3(b)) and the emission scattered from each end-facet was collected by the selected area spectral measurement system. By near field coupling a long CdSe NW and a 100 nm diameter Ag NW, they demonstrate a hybrid photon plasmon NW laser that offers subdiffraction limited beam size and spatially separated plasmon modes. The laser operates around 723 nm wavelength at room temperature and offers far field accessible pure plasmon cavity modes on a 3.7 μm long Ag NW with a beam size of 0.008 λ^2. They also show that the hybrid photon plasmon NW laser can be modulated by solely modifying the propagation loss of the plasmon modes in the Ag NW. When the pumping fluence increases from 27 to 97 μJ cm^{-2}, the emission output experiences a lasing spectrum shown in Figure 3(d).

Semiconductor nanostructures have major potential to be used as a critical component in compact optical devices at the nanoscale. The Fabry-Perot type of SPPs of laser amplification by nanostructure has been realized. It provides a lot of chances for the assembly of nanoscale electronic and

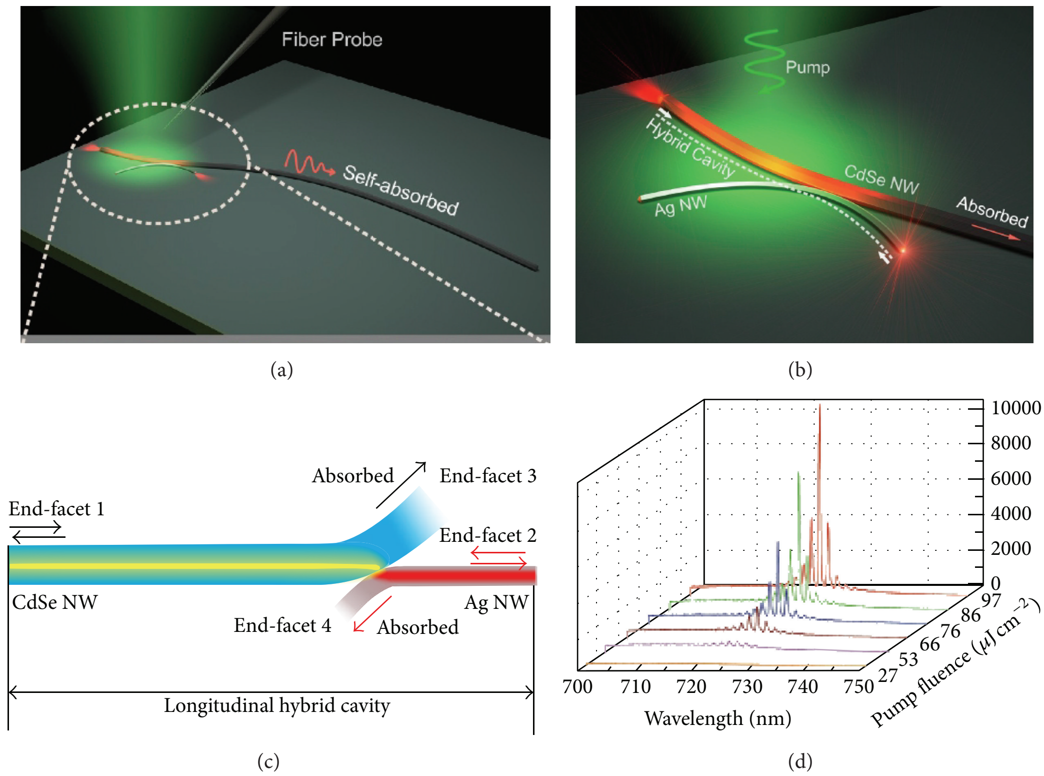

Figure 3: Schematic illustration of a hybrid photon-plasmon NW laser. (a) The hybrid photon-plasmon NW laser is composed of an Ag NW and an ultralong CdSe NW coupled into X-shape using a fiber probe for micromanipulation. The right segment of CdSe NW serves as a distributed absorber without reflection. (b) Closed-up view of the coupling area indicating the coupled hybrid cavity (marked by the dashed line), which serves as the hybrid photon-plasmon lasing cavity. (c) Cavity formation in the X-structure. (d) Lasing spectra collected from the Ag end-facet under pump fluences of 27–97 μJ cm^{-2}.

optoelectronic devices. What is more, these nanostructures demonstrate new and enhanced features crucial to several fields of technology.

3. Type of Gain Material

One of the attractive characters of plasmonic waveguides is their capacity to confine light lower than the traditional diffraction limit. However, the increase of mode confinement usually comes at the price of large propagation loss. SPPs propagating between metal and dielectric interface sustain propagation losses over several hundred cm^{-1} at visible wavelengths. The decrease of optical loss is of rather importance in metallic structures depending on surface plasma waves, for example, transmitting electromagnetic energy [2], realizing negative refraction [41]. Despite many improvements that can be achieved by means of the optimization of the geometry and materials and by reducing structural defectives, the optical losses are caused by the physical performances of the metal and can only be dealt with by introducing optical gain into the structure [22]. Adopting this project, a reduction in the loss of propagating plasmons using dye doped [32, 42], QDs [43, 44], Er ions [45, 46], or semiconductor [47] has been reported recently.

Generally, dyes are emitted in the visible and low (<1 μm) near infrared spectral range and have broad emission lines. The development of stimulated radiation at wavelengths above 1 μm is still a challenge due to the fact that polymer hosts usually suffer from absorption by vibrations of the C–H bond in the near infrared wavelength region. The QDs nanostructures with the radius in the range from 1 to 10 nm are synthesized by colloidal chemistry. In this case, the emission wavelength can be easily tuned by controlling the material of the dots and their sizes. They can be easily embedded in polymer matrices using a common solvent. Compared to the other two gain media discussed above, Er ion doped polymers have the advantages of emitting in the corresponding spectral ranges as well as producing emission within the 1310 nm and 1550 nm windows, which are important for telecommunication applications. Although several studies have applied gain medium to compensate for the optical loss of strongly confined SPPs, semiconductors tend to be the choice of materials for losses in excess of 1000 cm^{-1}. At infrared wavelengths, the loss of maximally confined hybrid SPPs is on the order of 1000 cm^{-1}, which is well within the gain range of a variety of common compound semiconductors. However, strong gain effects, such as gain guiding, could provide additional design freedoms for future devices.

3.1. Dyes. The coupling of fluorescence of dye with SPPs was subject to investigation [24, 30], and recently it found

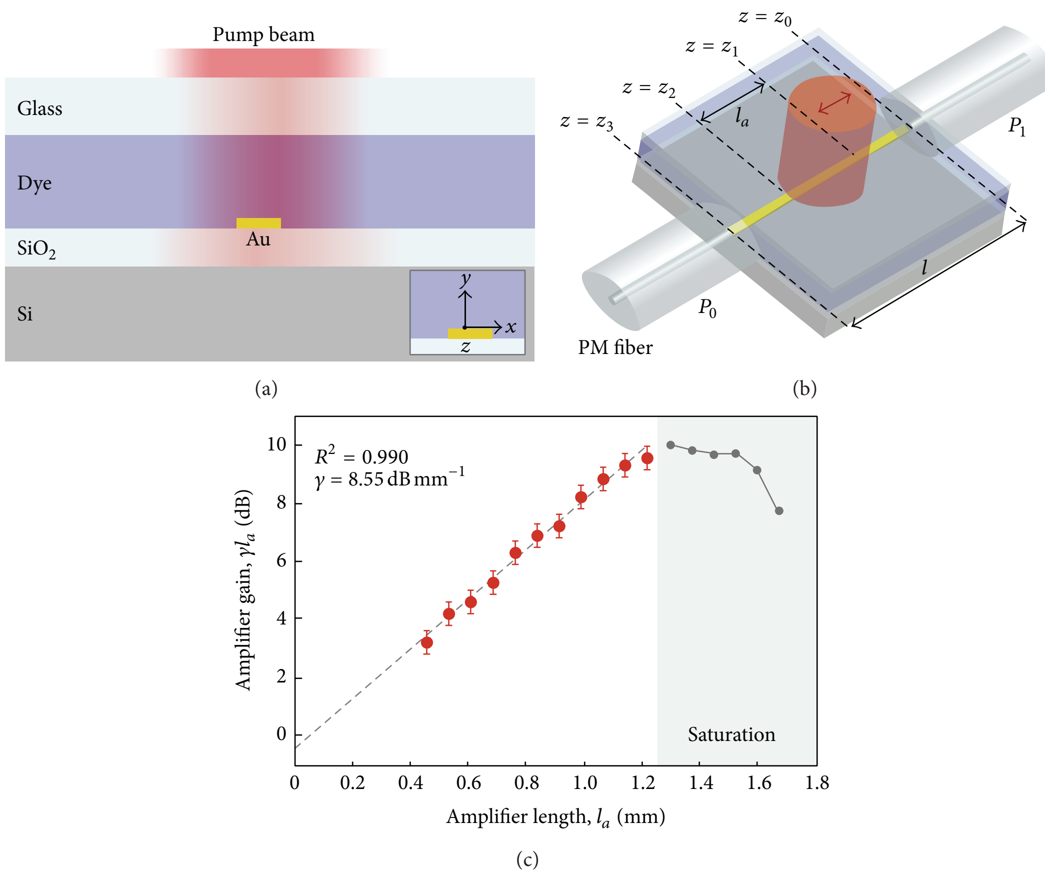

FIGURE 4: (a) Cross-sectional view of active structure. The gain medium is in the form of a laser dye in solution. Inset: coordinate system with the z-direction coming out of the page. (b) Pump and probe signal coupling arrangements used for amplification experiments. Pump polarization, indicated by the red arrow, is parallel to the waveguide length (z-axis). A probe signal is coupled in and out of the structure by means of end-fire coupling using polarization-maintaining (PM) fibers. (c) Measurements of amplifier gain versus amplifier length. A linear fit to the unsaturated data yields an LRSPP mode power gain of $\gamma = 20\,dB\,cm^{-1}$.

applications in fields such as plasmonic lasers [25] and surface plasmon enhanced fluorescence spectroscopy biosensors [26]. Fluorescence trapped in SPPs to far field radiation by adopting various methods [19–21] was reported to provide efficient means for collecting of enhanced SPPs signal. Dye has been considered as gain media for SPPs structure as proposed by Plotz et al. [23] in 1979 and has subsequently been reported by others. Avrutsky [48] demonstrated that dyes as a medium with strong gain are able to increase propagation length in silver films. Seidel et al. [49] experimentally demonstrated optically pumping a dye solution and using a prism coupling method by stimulated emission at 633 nm of SPPs in silver films. In recent works, the dielectric gain material consisted of dyes embedded into a polymer. Such a multicomponent material has the advantages of joining the active performances of the dyes with the technological feasibility of polymers. So de Leon and Berini [42] suggested a silver planar film surrounded by CYTOP and Rhodamine has been studied, demonstrating theoretically that for high enough powers and dye concentration amplification in the visible range is possible. The same dye dispersed in PMMA was investigated as a medium able to provide gain equal to $420\,cm^{-1}$ invested by Noginov et al. [31]. In these conditions, using the attenuated total reflection setup can compensate the losses of a silver film at 594 nm by nanocomposite. Then, the same authors [50] used a similar system to demonstrate stimulated emission of SPPs in the polymer film. Recently, Gather et al. [32] chose a fluorescent polymer made by the dispersion of PFS in MDMO-PPV obtaining a net optical gain of $8\,cm^{-1}$ at 600 nm in the SPPs. de Leon and Berini [25] first provided direct measurement of gain in propagating SPPs using the LRSPP supported by a symmetric metal stripe waveguide that incorporated optically pumped dye molecules as the gain medium. A cross-sectional view of the waveguide structure is shown in Figure 4(a). The gold stripe, which was 20 nm thick and 1 mm wide, lay on a 15 mm thick SiO_2 layer thermally grown on a silicon substrate and covered by a gain layer 100 mm thick consisting of optically pumped IR140 dye molecules. The dye was pumped at $\lambda_p = 808$ nm and the LRSPP was probed at $\lambda_e = 882$ nm close to the peak absorption and emission of the dye, respectively. The arrangement used for pumping and probing is depicted in Figure 4(c). The pump light was normally incident onto the top side of the structure linearly polarized along the

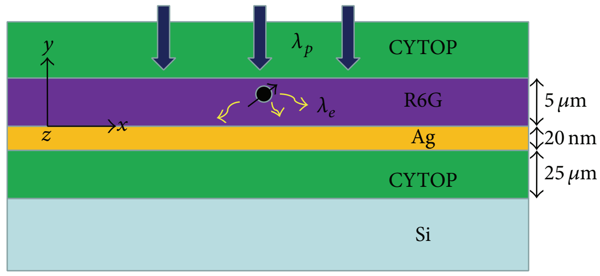

Figure 5: The SPP waveguide structure considered in the work.

z-axis (8 ns FWHM pulses, repetition rate of 10 Hz). Gain measurements were obtained as a function of the amplifier length l_a, as shown in Figure 4(c), from which the slope yields an LRSPP mode power gain of $\gamma = 20\,\text{dB cm}^{-1}$.

The same workers [42] considered another structure shown in Figure 5. It is made up with a silver film of 20 nm thick extending infinitely over the xz-plane. A lossless 25 μm thick dielectric CYTOP constitutes bottom cladding, sitting on a semi-infinite silicon substrate. The top surface is covered by R6G dye molecules in a mixture of ethanol and methanol. The dye solution is covered by a 5 μm thick semi-infinite CYTOP. A monochromatic pump signal of wavelength $\lambda_p = 532$ nm (near the peak absorption of R6G) is excited from the top of dye molecules. SPPs mode amplification is studied with the peak emission wavelength $\lambda_e = 560$ nm of the dye. The silver film in the vicinity normalized to the irradiance $I_p(y)$ of the incoming pump signal. The vertical dashed lines outline the silver film. The lower cladding thickness was used to reduce the resonant coupling to the slab mode. Owing to field reflection throughout the structure the irradiance follows a standing wave pattern in the dye. The population inversion is enhanced in those regions, achieving 2.5-fold maxima.

In general, the emission wavelength reported for dyes doped polymer is lower than 1000 nm, which falls within the telecommunication window. Dyes molecules as gain medium exciting the SPPs on the metal surface were presented as a mean of achieving SPPs compensation. A higher gain medium would be required because ohmic losses in metal at visible wavelengths are much greater than those at infrared wavelengths. Fluorescence emitted by dyes medium near the metallic surface couples with the SPPs. This process is efficient and collects emission with optical elements. The coupling between fluorescence emission of dyes and SPPs will have a broad range of applications.

3.2. QDs. SPPs ohmic losses in metallic nanostructure are the primary obstruction in acquiring excellent optical performance for photonic applications. Some measures have been proposed to polish up these losses including adopting gain media and parametric processes [51–59]. For dye gain media, Chénais and Forget [60] reported net modal gains achieve $100\,\text{cm}^{-1}$ in slab waveguide geometries in the visible range. Substantially greater material gain is usually referred to the QDs. For example, values up to $\approx 10^5\,\text{cm}^{-1}$ have been reported for saturation material gain in 1.3 μm emitting InGaAs QDs [61]. Compared with other organic dyes, QDs display more excellent photochemical stability in fluorescence applications. The surface modified QDs exhibit outstanding dispersibility in water, saline buffers, and in various pH conditions for more than 7 months. Moreover, the emission wavelength can be easily tuned by controlling the size or the base material. In this way optical amplification has already been demonstrated in dielectric waveguides with the QDs dispersed in it [62]. Besides, Surez et al. [63] mixed CdSe and CdTe QDs in PMMA, and the optimum conditions for waveguiding were obtained. Indeed, amplification of SPP using QDs PMMA nanocomposites has already been studied [43, 64]. PbS QDs are proposed as a method to provide gain in a dielectric load SPPs waveguide [64]. This structure consists of a dielectric strip deposited on a metal film, being possible to improve waveguiding characteristics by choosing parameters reasonably [14]. Then, a 32% compensation of SPP was demonstrated under the similar structure working at 876 nm [43]. Garcia et al. [44] obtained a 33% loss reduction in a dielectric loaded SPPs waveguide corresponding to $143\,\text{cm}^{-1}$ of optical gain, using QDs doped PMMA ridges.

Bolger et al. [65] reported PMMA films of below 1 μm thickness were spin coated onto the Au structures (Figure 6(a)). The polymer films were doped with PbS QDs and used as an amplifying medium. A 633 nm He-Ne laser (3 mW) was directed at the incoupling grating (G1) and excited the QDs photoluminescence at around 1160 nm that is coupled to the SPPs at the Au/polymer interface. According to the SPP intensity dependencies on the pump power for several sets of the in/outcoupling gratings with different distances between them, the dependence of the signal SPPs propagation length on the pump intensity can be reconstructed (Figure 6(b)). The propagation length increases at low pump intensities reaching the maximum of approximately a 30% increase at about $1\,\text{W/cm}^2$.

Grandidier et al. [64] investigated propagation assisted by stimulated emission in a polymer strip loaded plasmonic waveguide doped with QDs. They achieve 27% increase of the propagation length at telecom wavelength corresponding to a $160\,\text{cm}^{-1}$ optical gain coefficient. PbS QDs were inserted in a PMMA polymer strip waveguide fabricated on 40 ± 3 nm thick gold films (Figure 7(a)). Figure 7(c) shows the QDs spontaneous emission intensity versus pump power. As expected from spontaneous decay, this signal linearly increases with pump power.

Radko et al. [43] investigated a four-layer structure composed of a quartz substrate, a 50 nm thick gold film, a thin layer of PMMA which embedded PbS QDs, and air (Figure 8(a)). They demonstrated an optical gain of $\sim 200\,\text{cm}^{-1}$ for the mode under consideration, which corresponds to ~32% compensation of SPP loss. PbS QDs exhibited a fluorescence emission peak at 876 nm and were pumped at 532 nm with a continuous waveform laser beam focused on a spot with diameter $d \sim 13.8\,\mu$m (Figure 8(b)).

It is hoped that SPPs propagation lengths can be greatly increased with the gain medium which provide optical gain. To this end, a gain medium composed of polymer and QDs compound is presented with the aim of proposing a

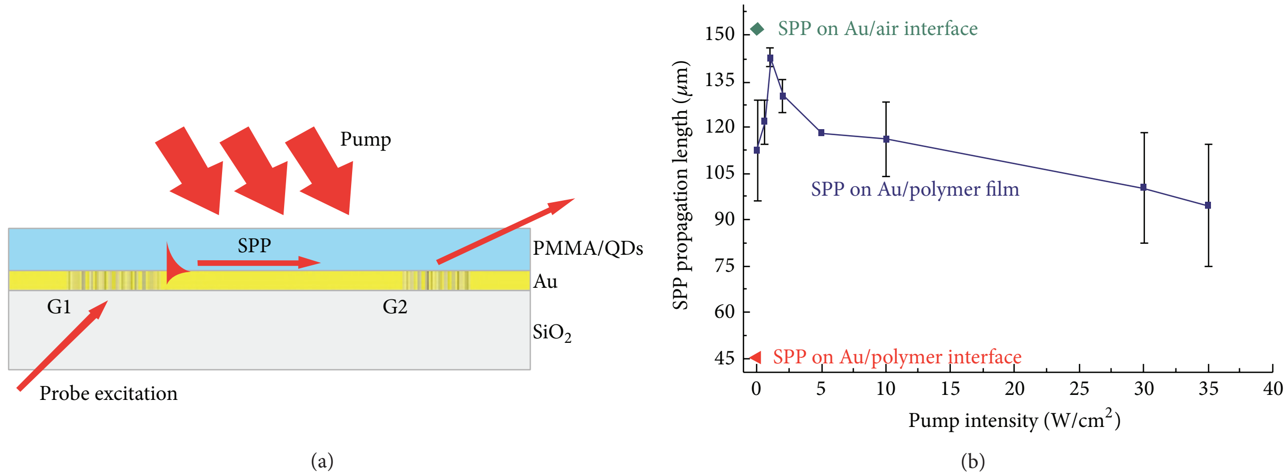

FIGURE 6: (a) Experimental setup for the optical measurements: a He-Ne laser light is coupled to SPPs on the G1 grating and excites signal SPPs via QD fluorescence. The amplifying medium is continuously pumped with a second He-Ne laser. The signal from the decoupling grating (G2) is collected into an optical fiber connected to the spectrometer. (b) The dependence of the propagation length of the signal SPPs on the pump intensity. The SPP propagation lengths on Au/semi-infinite polymer and Au/air interfaces are also shown.

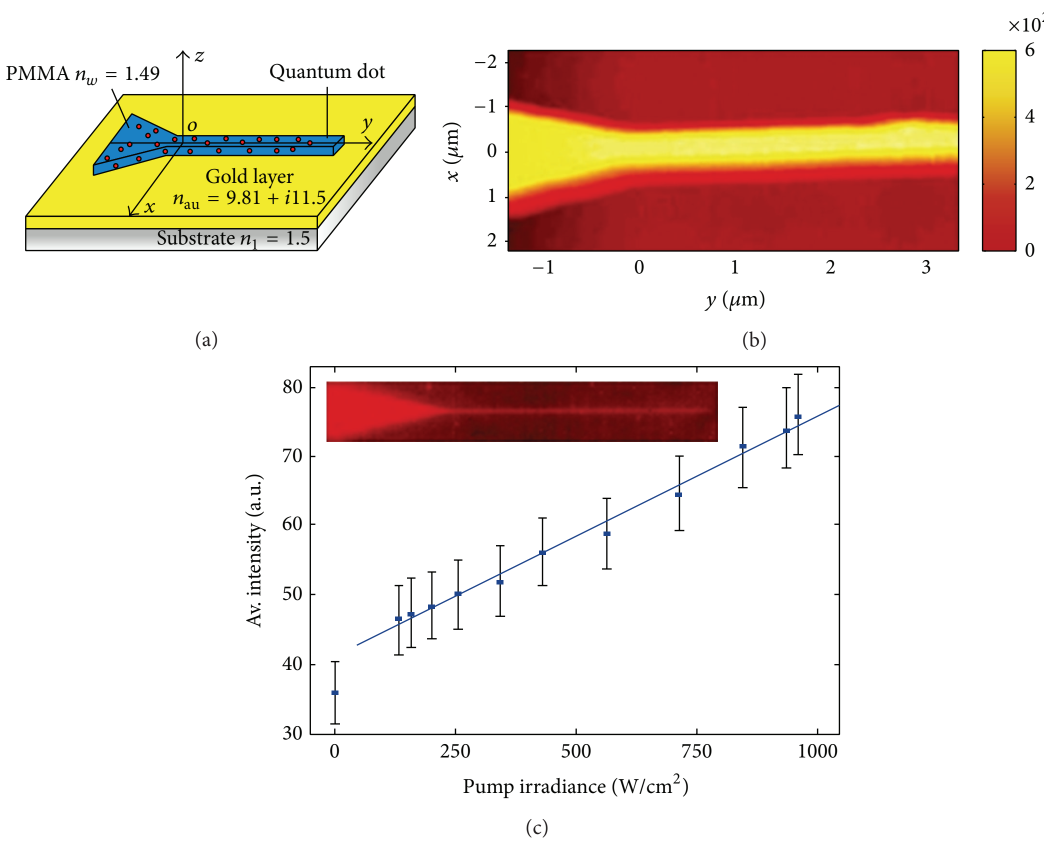

FIGURE 7: (a) Device configuration: a PMMA strip confines the plasmon at the gold/polymer interface. An additional tapering structure is designed to efficiently excite the SPP guided mode with an external infrared laser. The effective indices used in the numerical simulations are indicated on the figure. (b) Atomic force microscopy image of the DLSPPW. The dimensions of the waveguide are 600 nm height, 400 nm width,, and 65 μm length. (c) Averaged spontaneous emission intensity for increasing pump powers (dots, standard deviation indicated) with a linear regression (blue line). The inset shows a homogeneous emission inside the waveguide since an extended illumination was used.

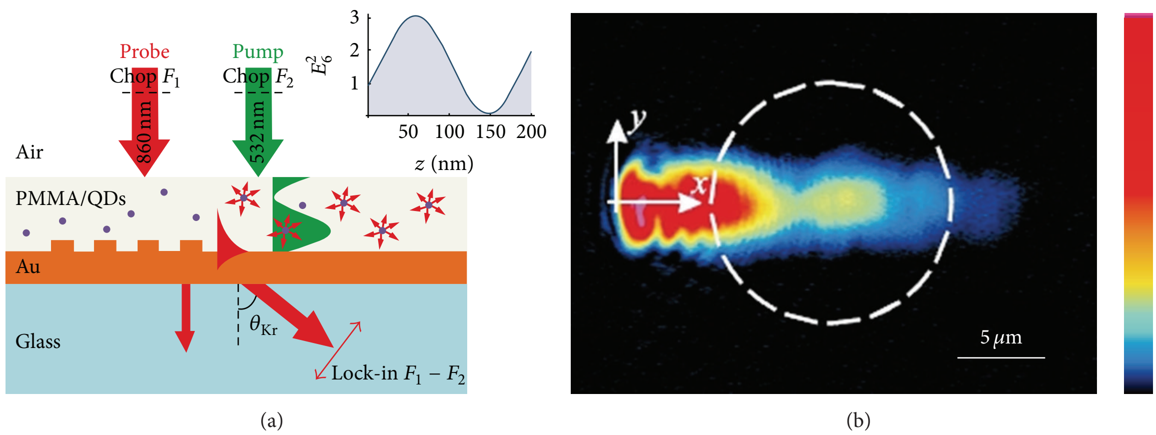

Figure 8: (a) Experimental configuration: thin PMMA film doped with PbS QDs on top of a 50 nm thick gold film. Excitation of a probe SPP beam ($\lambda = 860$ nm) is achieved through a grating. Inset shows a calculated distribution of the intensity of the pump beam ($\lambda = 532$ nm) inside the PMMA layer. (b) Leakage-radiation microscopy image of a probe SPP beam. The dashed circle shows the position where the pump beam is focused.

technologically feasible material which can tune the amplified wavelength by altering the nanostructure. Hence, wavelength tunability of the stimulated radiation (400 nm~2 μm) can be achieved by changing the material and the size of the QDs.

3.3. Erbium Ion. Rare earth elements have potential optoelectronic applications due to their performance of photoluminescence and electroluminescence embedded in a solid state matrix [66]. Visible emissions of the Er ions in wide band gap semiconductors were intensively investigated. Er ions played an important role in optical communication systems operating at 1500 nm. At a certain temperature the Er emission spectrum was fixed for a given material because of the absorption and emission spectra of Er determined by Boltzmann distributions [67]. Many applications of materials doped Er ions depend mainly on the exact line shape of the emission. It would be very interesting if the Er emission spectrum could be externally modified. Previously, the energy transfer between the Er ions and the SPPs at the interface of metal and silica had been demonstrated by Kalkman et al. [46]. He also reported that emission spectra close to optical communication wavelength could be modified by grating structures due to SPPs reradiated into far field [67]. Then, Wang and Zhou [68] proposed a double grating configuration that greatly strengthened the emission of Er ions. The emission efficiency of the Er ions at 1550 nm increased more than ten times than other emission wavelengths within the 1500 nm communication windows, since the maximum density of the states of the SPPs was localized at the edge of the band edges [69–71]. Wang also proposed a silicon optical amplifier based on SPPs enhancement. The gain coefficient of the Si: SiEr-metal-silicon structure increased 24% at 1540 nm and the loss sharply reduced compared with a conventional stack structure [72]. In addition, the luminescence intensity of Er ions can be enhanced, when they are localized or close to nanoparticles (NPs), which is termed as SPPs enhanced luminescence [17, 73]. Christensen et al. [74] demonstrated the upconversion luminescence of Er ions doped materials in the TiO_2:Er^{3+} system when Au NPs were in close vicinity to the Er ions.

Verhagen et al. [75] studied the field enhancement and found that it was ascribed to the excitation of both propagating and localized surface plasmon resonances in arrays of square and annular apertures in an Au film. The measurement geometry was schematically depicted in Figure 9(a). The Er ions can convert infrared radiation with a free space wavelength of 1480 nm to emission at shorter wavelengths through an upconversion process. A level diagram of the 4f energy levels in Er^{3+} was shown in Figure 9(b).

Ambati et al. [45] reported a direct experimental evidence of stimulated emission of SPPs at telecom wavelengths (1532 nm) with Er doped by glass as a gain medium. They observed an increase in the propagation length of signal SPPs when Er ions were excited optically using pump SPPs. The experimental setup was developed to accommodate the optical pumping of Er doped with glass by using LRSPP mode guided by the same metal strip shown in Figure 10(a). A laser diode with nominal wavelength of 1480 nm was used as the pump and a different laser diode at 1532 nm signal was used as the signal. However, in continuous wave mode, a maximum signal enhancement of ~50% (1.73 dB) was recorded at a higher pump power of 266 mW (Figure 10(b)).

Lots of researchers studied that the Er ions were excited in wide band gap semiconductors because Er ions played an important role in optical communication system operating at 1500 nm. In addition, at a certain temperature the Er emission spectrum was fixed for a given material because of the absorption and emission spectra of Er determined by Boltzmann distributions. As a result, there was a significant promise of the SPPs-assisted Er ions light emission.

3.4. Semiconductor. Due to the outstanding properties, resonance cavities with semiconductor as optics compensation have attracted growing interests in constructing nanoscale photonic and optoelectronic devices and circuits [35, 36]. Generally, a semiconductor cavity with the round trip gain,

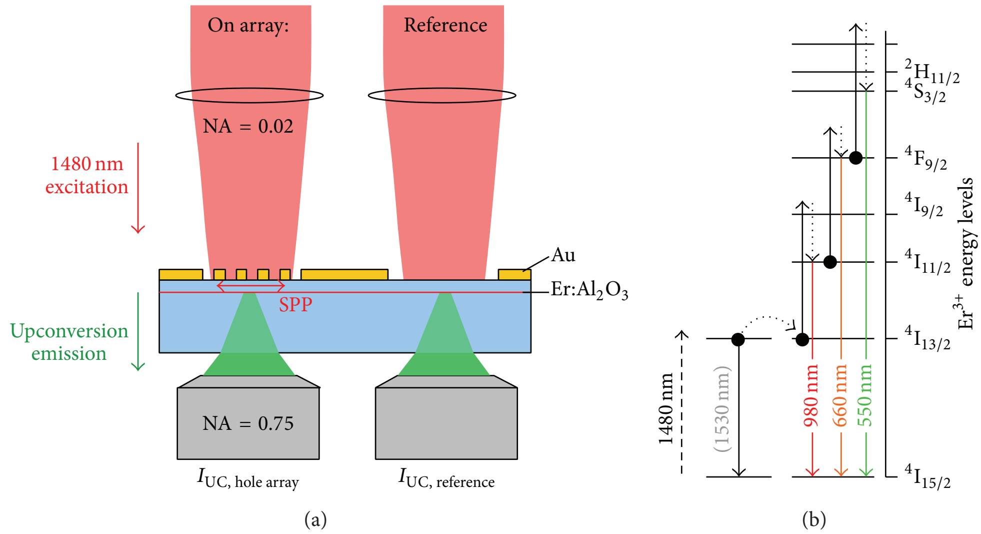

FIGURE 9: (a) Schematic depiction of the measurement geometry. The sample is illuminated with 1480 nm pump light, and upconversion luminescence from Er ions implanted in the sapphire substrate is collected through the substrate. (b) Er^{3+} 4f level diagram indicating the upconversion mechanism that leads to the population of Er^{3+} levels emitting at wavelengths of 980, 660, and 550 nm under 1480 nm excitation.

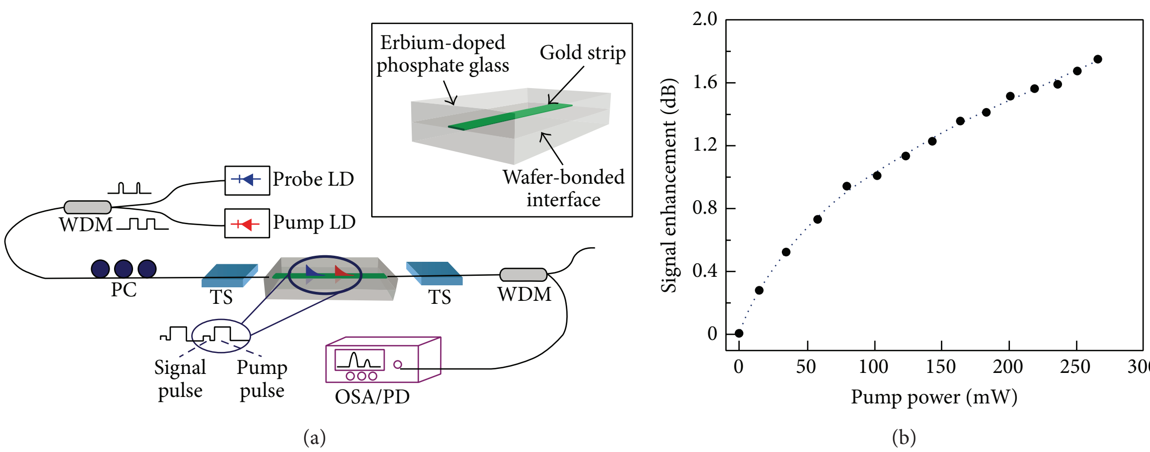

FIGURE 10: (a) Experimental configuration for inducing stimulated emission of SPPs, (b) enhancement of the signal as a function of pump power in continuous mode.

sustained by a certain feedback such as end-face reflection, can compensate round trip losses. Typically, the semiconductor cavity of this kind was formed by end-face reflection [76–79] or ring resonance [80, 81]. Hill et al. [82] introduced a metalized, etched semiconductor heterostructure as shown in Figure 11(a). SPPs between the two metal planes were weakly confined by a small index variation along the heterostructure's growth direction leading to that guided wave propagation paralleled to the plane of the substrate. The thinnest heterostructure reported in this work was just 90 nm thick resulting in SPPs smaller than the diffraction limit in one dimension. A Fabry-Perot SPPs resonator consisted of the end-facets of the metalized structure.

Another device reported by Oulton and coworkers [33] also used a Fabry-Perot cavity, but with plasmonic confinement in two dimensions perpendicular to wave propagation. The laser cavity consists of a semiconductor nanowire put on a flat metal film with a thin nanoscale insulating gap, as shown in Figure 12(b). Remarkably, the mode of the NW and the SPPs of the metal surface hybridized into a deep subwavelength mode propagating along the wire's axis. Here, a small amount of feedback was provided by the end-facets of the NW forming a cavity.

Ma et al. [83] reported another kind of semiconductor cavity operating at room temperature with $\lambda/20$ optical confinement (Figure 13). A 45 nm thick CdS nanosquare atop a silver surface separated by a 5 nm thick magnesium fluoride gap layer provided the subdiffraction limited mode confinement and low metal loss. Surprisingly, although the high index material is only 45 nm thick, the SPPs of this system carry high momentum even higher than light waves in bulk CdS or plasmonic NW lasers. This leads to strong

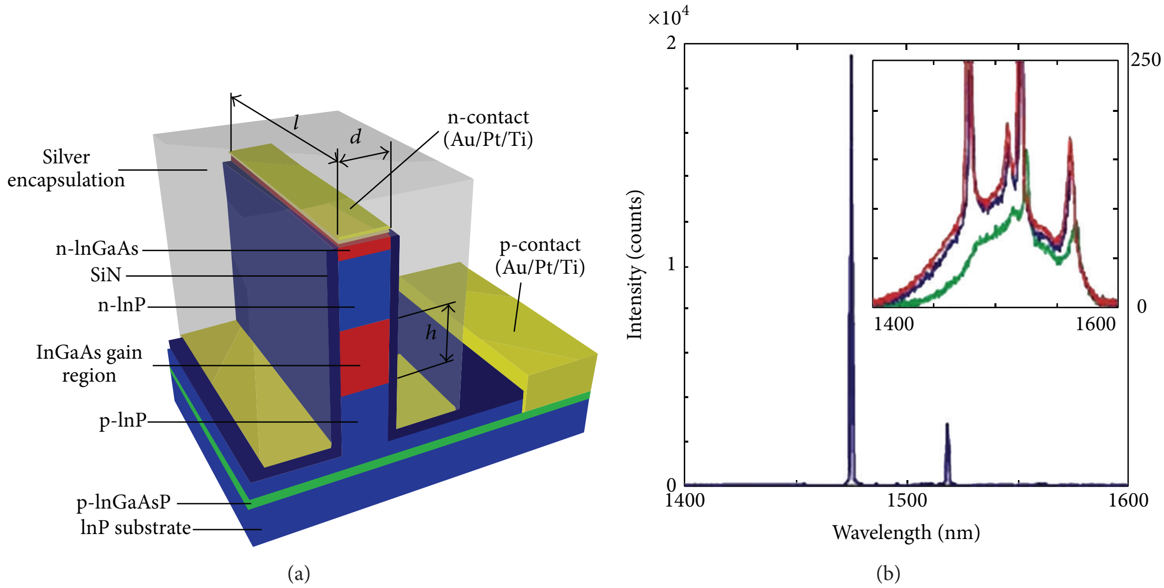

FIGURE 11: (a) Schematic showing the device layer structure. (b) Spectra and near field patterns showing lasing in devices. Above threshold emission spectrum for 3-micron-long device with semiconductor core width of $d \sim 130$ nm (± 20 nm), with pump current of 180 μA at 78 K. Inset: emission spectra, for 20 (green), 40 (blue), and 60 (red) μA, all at 78 K.

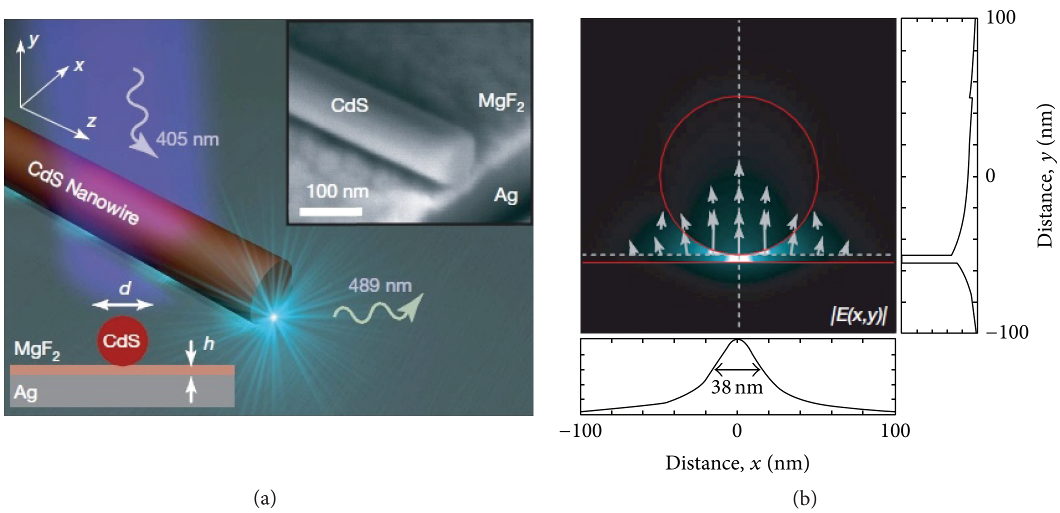

FIGURE 12: (a) The plasmonic laser consists of a CdS semiconductor nanowire on top of a silver substrate separated by a nanoscale MgF_2 layer of thickness h. This structure supports a new type of plasmonic mode, the mode size of which can be a hundred times smaller than a diffraction-limited spot. The inset shows a scanning electron microscope image of a typical plasmonic laser, which has been sliced perpendicular to the nanowire's axis to show the underlying layers. (b) The stimulated electric field distribution and direction $|E(x, y)|$ of a hybrid plasmonic mode at a wavelength of 489 nm, corresponding to the CdS I_2 excitonline. The cross-sectional field plots (along the broken lines in the field map) illustrate the strong overall confinement in the gap region between the nanowire and metal surface with sufficient modal overlap in the semiconductor to facilitate gain.

feedback through total internal reflection of surface plasmons at the cavity boundaries.

The interaction between SPPs and semiconductors at nanoscale is becoming the research focus in the fundamental physics. The amplification based on semiconductor nanostructure has been experimentally demonstrated. Three characters (small size, high refractive index, and free standing nanocavity emit) make semiconductor nanostructure attractive for potential application in optoelectronics. A further side of this theme is the overcoming of large propagation losses in nanoscale plasmon mode waveguides, creating nanolasers from these waveguides. These lasers will be very important for complex optoelectronics systems in future.

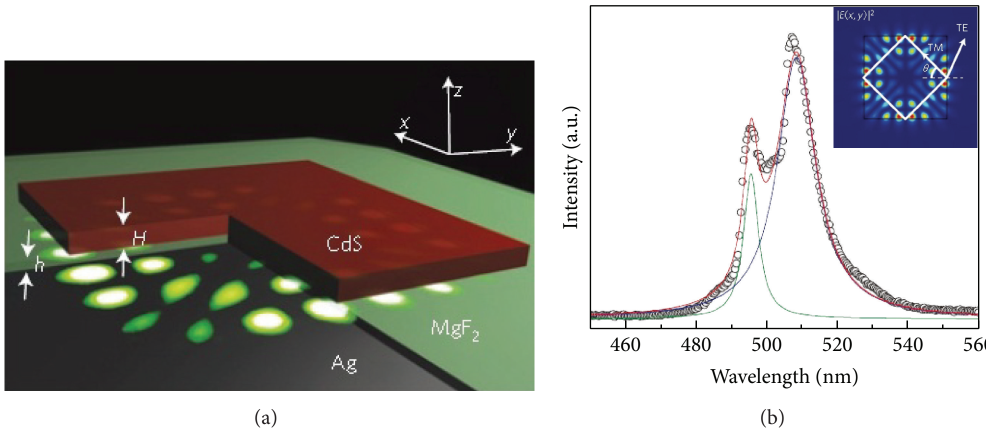

FIGURE 13: (a) Schematic diagram of the room-temperature plasmon laser showing a thin CdS square atop a silver substrate separated by a 5 nm MgF_2 gap, where the most intense electric fields of the device reside. (b) The spontaneous emission spectrum at a peak pump intensity of 1,960 MW cm^{-2} shows obvious cavity modes despite being below the threshold, which indicates the excellent cavity feedback. The inset shows electric-field-intensity distribution of a TM mode in the x and y directions.

4. Applications of SPPs under Gain Compensation

SPPs, which are electromagnetic waves strongly confined in the direction perpendicular to the metal surface, have the unique ability to concentrate and guide light in subwavelength scale [2, 84]. This certainly provides an abundant basis for studies of light matter interaction at the nanoscale. However, the strong SPPs optical losses are impeded largely for many practical applications, and loss compensation with optical gain will in many cases be feasible when it comes to the design of functional devices.

4.1. Lasers. The construction of a plasmonic laser is similar to that of a conventional laser. SPPs are directly generated on a metal nanostructure and amplified by an adjacent dielectric medium incorporating gain, while a feedback mechanism allows SPPs to resonate. The gain medium amplifies SPPs by stimulating emission of radiation generating coherently amplified light that is bound to the metal dielectric interface and typically cannot escape without coupling optics. The involvement of electrons in the SPPs adds momentum to light, confining it closely to the metal. This confinement effect is used by plasmonic lasers to deliver strong optical energy well below the diffraction barrier on extremely fast time scales. Bergman and Stockman proposed the coupling of energy directly into SPPs by emission for fast and efficient light generation at the nanoscale in 2003 [85]. But their concept was not carried out experimentally until 2009 [33, 82, 86, 87]. There have also been recent works on the amplification and laser action of SPPs. Room-temperature operation has been reported for LRSPP exhibiting low confinement [32, 88, 89] and for tightly confined hybrid SPPs [90]. Meanwhile, the work of Hill and coworkers continued to pioneer electrically injected plasmon lasers [91, 92]. The laser action which can directly generate SPPs has been adapted to commercial lasers. For example, metallic nanostructures have been positioned on the facets of commercial quantum cascade lasers leading to the strong nanofocusing applied in antennas [93] and the control of beam directionality used as arrays of slits and gratings [94–96].

4.2. Amplifiers. Substantial efforts have been applied to study the amplification of SPPs [25, 32, 49, 65, 97–99] targeting to mitigate or even eliminate their large intrinsic losses in order to enable full potential applications in SPPs. Indeed, the direct observation of SPPs amplification in confined waveguide geometries is elusive. Kéna-Cohen et al. [100] reported the direct observation of plasmonic amplification in confined and lithographically defined SPPs waveguides of varying length. At the highest pump powers, they found that the SPPs loss was completely compensated by the optically pumped organic gain medium and resulted in a substantial net gain of 93 dB/mm for the best amplifier. de Leon and Berini [101] measured the amplified spontaneous emission in a LRSPP amplifier at a near infrared wavelength and found an effective input noise power of photons per mode. Then, they also presented a theoretical and numerical study of the noise properties of high gain planar SPPs amplifiers combined with dipolar gain media [102]. On this basis, they showed a theoretical study of gain and noise in a LRSPP amplifier which consisted of a symmetric thin metal film with an optically pumped gain medium [103]. The amplifier structure was shown in Figure 14. It consisted of a 20 nm thick gold film deposited on a semi-infinite SiO_2 substrate and covered by a gain medium in the form of optically pumped LDS821 dye molecules. A semi-infinite SiO_2 within a 1 mm thick layer was covered on the dye. The structure was pumped from the top using monochromatic light with a wavelength of $\lambda_p = 532$ nm which was close to the dye's peak absorption. The amplification of SPPs sets up the foundation for many interesting, useful, and compelling applications; for instance, SPP amplifiers can be used as components integrated with plasmonic elements, biosensors, or circuitry to compensate for losses or otherwise brilliance characteristics.

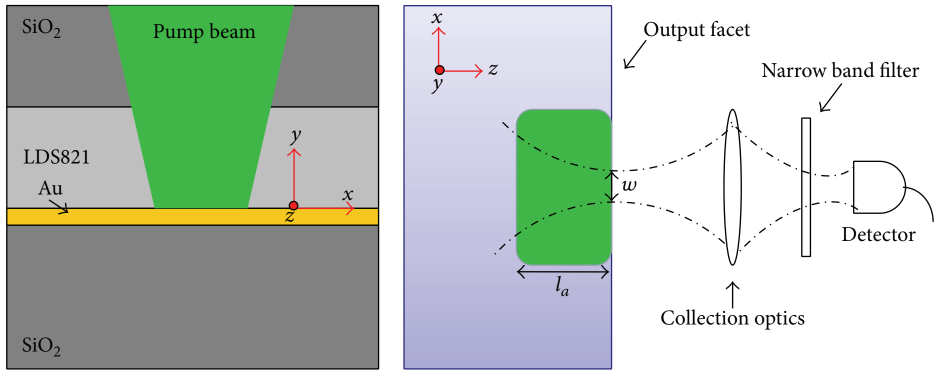

(a) (b)

FIGURE 14: LRSPP amplifier structure: (a) front cross-sectional view. (b) Top view and detection system.

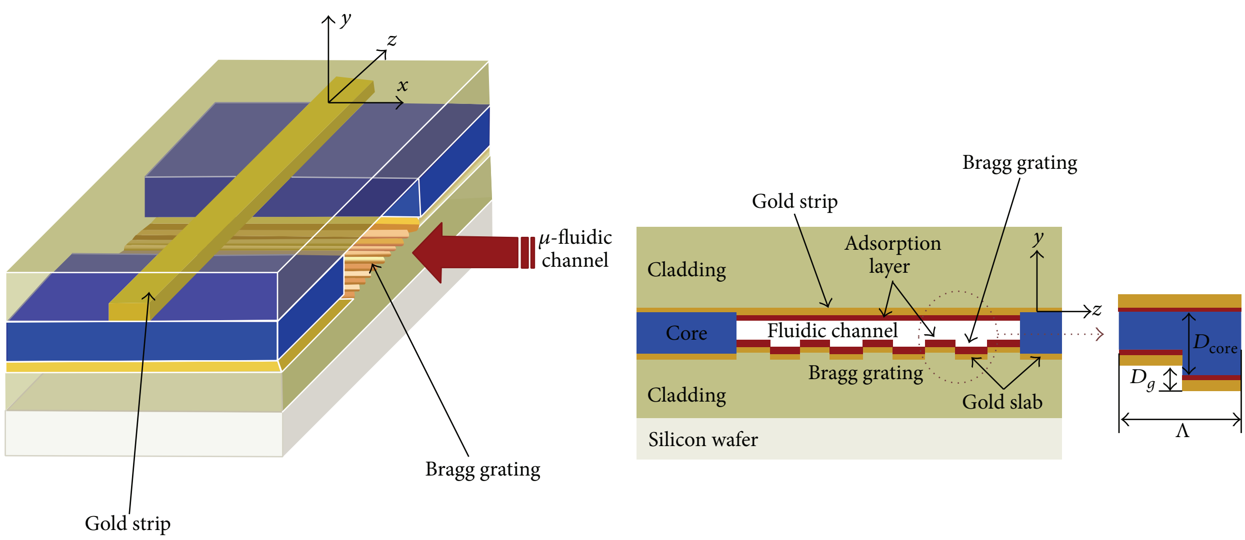

(a) (b)

FIGURE 15: (a) A schematic of LRSPP waveguide sensor, (b) cross-sectional views of the sensor structure.

4.3. LRSPP Waveguide. In recent years, the LRSPP excited at the interfaces of metal thin films embedded in a gain medium have generated significant research interest. In terms of potential uses of SPPs waveguides, the strength of the limitation is an urgent issue. Theoretical and experimental [104, 105] studies have demonstrated that a long range mode can be propagated in single polarization over a distance of several μm in a simple structure composed of a thin metal strip embedded in dielectric materials. For LRSPP waveguides, single polarization operation and the high precision can be achieved in patterning the waveguide core layer contributing to high performance of LRSPP based quantum optical circuits. Fabrication of active and passive optical components, including Y-splitters, directional couplers, switch, attenuators, sensor, and Mach-Zehnder wavelength filters, has been demonstrated by several groups [105–109] (Figure 15).

5. Conclusion

The presence of SPPs in metallic nanostructures relates to a variety of unique optical effects. But in many cases, optical losses greatly limit the applicability of plasmonic technologies as a means of realizing. This obstacle can be overcome by adding optical gain to compensate for loss alters and allow SPPs to propagate over longer distances. In this review, we showed the two SPPs optical amplification mechanisms including spontaneous radiation amplification and simulated radiation amplification. Many improvements can be achieved by means of the optimization of the geometry and materials, but the optical losses are caused by the physical performances of the metal and can well be dealt with by introducing optical gain into the structure. Then, we introduced several gain mediums, such as dye doped, QDs, erbium ion, and semiconductor, to compensate optical loss of SPPs. Using gain medium mentioned above can compensate losses and achieve many potential applications, for example, laser, amplifier, and LRSPP. In the future, SPPs geometries with a range of gain material have been shown to provide a suitable platform for the study of net plasmon amplification and will lead to useful and helpful applications.

Conflict of Interests

The authors declare that there is no conflict of interests regarding the publication of this paper.

Acknowledgments

This work is supported by NSFC under Grant no. 61307066, Doctoral Fund of Ministry of Education of China under Grant nos. 20110092110016 and 20130092120024, Natural Science Foundation of Jiangsu Province under Grant no. BK20130630, the National Basic Research Program of China (973 Program) under Grant no. 2011CB302004, and the Foundation of Key Laboratory of Micro-Inertial Instrument and Advanced Navigation Technology, Ministry of Education, China, under Grant no. 201204.

References

[1] W. L. Barnes, "Surface plasmon-polariton length scales: a route to sub-wavelength optics," *Journal of Optics A: Pure and Applied Optics*, vol. 8, no. 4, pp. S87–S93, 2006.

[2] W. L. Barnes, A. Dereux, and T. W. Ebbesen, "Surface plasmon subwavelength optics," *Nature*, vol. 424, no. 6950, pp. 824–830, 2003.

[3] S. A. Maier and H. A. Atwater, "Plasmonics: localization and guiding of electromagnetic energy in metal/dielectric structures," *Journal of Applied Physics*, vol. 98, no. 1, Article ID 011101, 2005.

[4] C. L. Haynes, A. D. McFarland, and R. P. van Duyne, "Surface-enhanced: raman spectroscopy," *Analytical Chemistry*, vol. 77, no. 17, pp. 338A–346A, 2005.

[5] D. K. Gramotnev and S. I. Bozhevolnyi, "Plasmonics beyond the diffraction limit," *Nature Photonics*, vol. 4, no. 2, pp. 83–91, 2010.

[6] S. Kawata, Y. Inouye, and P. Verma, "Plasmonics for near-field nano-imaging and superlensing," *Nature Photonics*, vol. 3, no. 7, pp. 388–394, 2009.

[7] J. N. Anker, W. P. Hall, O. Lyandres, N. C. Shah, J. Zhao, and R. P. van Duyne, "Biosensing with plasmonic nanosensors," *Nature Materials*, vol. 7, no. 6, pp. 442–453, 2008.

[8] J. Homola, "Surface plasmon resonance sensors for detection of chemical and biological species," *Chemical Reviews*, vol. 108, no. 2, pp. 462–493, 2008.

[9] T. W. Ebbesen, C. Genet, and S. I. Bozhevolnyi, "Surface-plasmon circuitry," *Physics Today*, vol. 61, no. 5, pp. 44–50, 2008.

[10] P. Berini and I. de Leon, "Surface plasmon-polariton amplifiers and lasers," *Nature Photonics*, vol. 6, no. 1, pp. 16–24, 2012.

[11] J. B. Khurgin and A. Boltasseva, "Reflecting upon the losses in plasmonics and metamaterials," *MRS Bulletin*, vol. 37, no. 8, pp. 768–779, 2012.

[12] R. Charbonneau, P. Berini, E. Berolo, and E. Lisicka-Shrzek, "Experimental observation of plasmon-polariton waves supported by a thin metal film of finite width," *Optics Letters*, vol. 25, no. 11, pp. 844–846, 2000.

[13] P. Berini, "Long-range surface plasmon-polariton waveguides in silica," *Journal of Applied Physics*, vol. 102, no. 5, Article ID 053105, 2007.

[14] T. Holmgaard and S. I. Bozhevolnyi, "Theoretical analysis of dielectric-loaded surface plasmon-polariton waveguides," *Physical Review B*, vol. 75, no. 24, Article ID 245405, 2007.

[15] M. Seidel and R. Niessner, "Automated analytical microarrays: a critical review," *Analytical and Bioanalytical Chemistry*, vol. 391, no. 5, pp. 1521–1544, 2008.

[16] M. E. Stewart, C. R. Anderton, L. B. Thompson et al., "Nanostructured plasmonic sensors," *Chemical Reviews*, vol. 108, no. 2, pp. 494–521, 2008.

[17] J. R. Lakowicz, "Plasmonics in biology and plasmon-controlled fluorescence," *Plasmonics*, vol. 1, no. 1, pp. 5–33, 2006.

[18] J. Dostálek and W. Knoll, "Biosensors based on surface plasmon-enhanced fluorescence spectroscopy," *Biointerphases*, vol. 3, no. 3, pp. FD12–FD22, 2008.

[19] J. R. Lakowicz, J. Malicka, I. Gryczynski, and Z. Gryczynski, "Directional surface plasmon-coupled emission: a new method for high sensitivity detection," *Biochemical and Biophysical Research Communications*, vol. 307, no. 3, pp. 435–439, 2003.

[20] J. S. Yuk, M. Trnavsky, C. McDonagh, and B. D. MacCraith, "Surface plasmon-coupled emission (SPCE)-based immunoassay using a novel paraboloid array biochip," *Biosensors and Bioelectronics*, vol. 25, no. 6, pp. 1344–1349, 2010.

[21] S. C. Kitson, W. L. Barnes, and J. R. Sambles, "Photoluminescence from dye molecules on silver gratings," *Optics Communications*, vol. 122, no. 4–6, pp. 147–154, 1996.

[22] A. N. Sudarkin and P. A. Demkovich, "Excitation of surface electromagnetic waves on the boundary of a metal with an amplifying medium," *Soviet Physics—Technical Physics*, vol. 34, pp. 764–766, 1989.

[23] G. A. Plotz, H. J. Simon, and J. M. Tucciarone, "Enhanced total reflection with surface plasmons," *Journal of the Optical Society of America*, vol. 69, no. 3, pp. 419–422, 1979.

[24] T. Okamoto, J. Simonen, and S. Kawata, "Plasmonic crystal for efficient energy transfer from fluorescent molecules to long-range surface plasmons," *Optics Express*, vol. 17, no. 10, pp. 8294–8301, 2009.

[25] I. de Leon and P. Berini, "Amplification of long-range surface plasmons by a dipolar gain medium," *Nature Photonics*, vol. 4, no. 6, pp. 382–387, 2010.

[26] A. Kasry and W. Knoll, "Long range surface plasmon fluorescence spectroscopy," *Applied Physics Letters*, vol. 89, no. 10, Article ID 101106, 2006.

[27] J. Dostálek, A. Kasry, and W. Knoll, "Long range surface plasmons for observation of biomolecular binding events at metallic surfaces," *Plasmonics*, vol. 2, no. 3, pp. 97–106, 2007.

[28] Y. Wang, A. Brunsen, U. Jonas, J. Dostálek, and W. Knoll, "Prostate specific antigen biosensor based on long range surface plasmon-enhanced fluorescence spectroscopy and dextran hydrogel binding matrix," *Analytical Chemistry*, vol. 81, no. 23, pp. 9625–9632, 2009.

[29] Y. Wang, J. Dostálek, and W. Knoll, "Long range surface plasmon-enhanced fluorescence spectroscopy for the detection of aflatoxin M_1 in milk," *Biosensors and Bioelectronics*, vol. 24, no. 7, pp. 2264–2267, 2009.

[30] G. Winter, S. Wedge, and W. L. Barnes, “Can lasing at visible wavelengths be achieved using the low-loss long-range surface plasmon-polariton mode?” *New Journal of Physics*, vol. 8, no. 8, article 125, 2006.

[31] M. A. Noginov, G. Zhu, M. Mayy, B. A. Ritzo, N. Noginova, and V. A. Podolskiy, “Stimulated emission of surface plasmon polaritons,” *Physical Review Letters*, vol. 101, no. 22, Article ID 226806, 2008.

[32] M. C. Gather, K. Meerholz, N. Danz, and K. Leosson, “Net optical gain in a plasmonic waveguide embedded in a fluorescent polymer,” *Nature Photonics*, vol. 4, no. 7, pp. 457–461, 2010.

[33] R. F. Oulton, V. J. Sorger, T. Zentgraf et al., “Plasmon lasers at deep subwavelength scale,” *Nature*, vol. 461, no. 7264, pp. 629–632, 2009.

[34] R. F. Oulton, V. J. Sorger, D. A. Genov, D. F. P. Pile, and X. Zhang, “A hybrid plasmonic waveguide for subwavelength confinement and long-range propagation,” *Nature Photonics*, vol. 2, no. 8, pp. 496–500, 2008.

[35] Y. Li, F. Qian, J. Xiang, and C. M. Lieber, “Nanowire electronic and optoelectronic devices,” *Materials Today*, vol. 9, no. 10, pp. 18–27, 2006.

[36] R. Yan, D. Gargas, and P. Yang, “Nanowire photonics,” *Nature Photonics*, vol. 3, no. 10, pp. 569–576, 2009.

[37] H. Ditlbacher, A. Hohenau, D. Wagner et al., “Silver nanowires as surface plasmon resonators,” *Physical Review Letters*, vol. 95, no. 25, Article ID 257403, 2005.

[38] P. Kusar, C. Gruber, A. Hohenau, and J. R. Krenn, “Measurement and reduction of damping in plasmonic nanowires,” *Nano Letters*, vol. 12, no. 2, pp. 661–665, 2012.

[39] N. Liu, H. Wei, J. Li et al., “Plasmonic amplification with ultrahigh optical gain at room temperature,” *Scientific Reports*, vol. 3, article 1967, 2013.

[40] X. Wu, Y. Xiao, C. Meng et al., “Hybrid photon-plasmon nanowire lasers,” *Nano Letters*, vol. 13, no. 11, pp. 5654–5659, 2013.

[41] J. Valentine, S. Zhang, T. Zentgraf et al., “Three-dimensional optical metamaterial with a negative refractive index,” *Nature*, vol. 455, no. 7211, pp. 376–379, 2008.

[42] I. de Leon and P. Berini, “Theory of surface plasmon-polariton amplification in planar structures incorporating dipolar gain media,” *Physical Review B*, vol. 78, no. 16, Article ID 161401, 2008.

[43] I. P. Radko, M. G. Nielsen, O. Albrektsen, and S. I. Bozhevolnyi, “Stimulated emission of surface plasmon polaritons by lead-sulphide quantum dots at near infra-red wavelengths,” *Optics Express*, vol. 18, no. 18, pp. 18633–18641, 2010.

[44] C. Garcia, V. Coello, Z. Han, I. P. Radko, and S. I. Bozhevolnyi, “Partial loss compensation in dielectric-loaded plasmonic waveguides at near infra-red wavelengths,” *Optics Express*, vol. 20, no. 7, pp. 7771–7776, 2012.

[45] M. Ambati, S. H. Nam, E. Ulin-Avila, D. A. Genov, G. Bartal, and X. Zhang, “Observation of stimulated emission of surface plasmon polaritons,” *Nano Letters*, vol. 8, no. 11, pp. 3998–4001, 2008.

[46] J. Kalkman, L. Kuipers, A. Polman, and H. Gersen, “Coupling of Er ions to surface plasmons on Ag,” *Applied Physics Letters*, vol. 86, no. 4, Article ID 041113, 2005.

[47] M. P. Nezhad, A. Simic, O. Bondarenko et al., “Room-temperature subwavelength metallo-dielectric lasers,” *Nature Photonics*, vol. 4, no. 6, pp. 395–399, 2010.

[48] I. Avrutsky, “Surface plasmons at nanoscale relief gratings between a metal and a dielectric medium with optical gain,” *Physical Review B*, vol. 70, no. 15, Article ID 155416, 2004.

[49] J. Seidel, S. Grafström, and L. Eng, “Stimulated emission of surface plasmons at the interface between a silver film and an optically pumped dye solution,” *Physical Review Letters*, vol. 94, no. 17, Article ID 177401, 2005.

[50] M. A. Noginov, V. A. Podolskiy, G. Zhu et al., “Compensation of loss in propagating surface plasmon polariton by gain in adjacent dielectric medium,” *Optics Express*, vol. 16, no. 2, pp. 1385–1392, 2008.

[51] A. B. Kozyrev, H. Kim, and D. W. van der Weide, “Parametric amplification in left-handed transmission line media,” *Applied Physics Letters*, vol. 88, no. 26, Article ID 264101, 2006.

[52] A. K. Popov and V. M. Shalaev, “Compensating losses in negative-index metamaterials by optical parametric amplification,” *Optics Letters*, vol. 31, no. 14, pp. 2169–2171, 2006.

[53] A. D. Boardman, Y. G. Rapoport, N. J. King, and V. N. Malnev, “Creating stable gain in active metamaterials,” *Journal of the Optical Society of America B: Optical Physics*, vol. 24, no. 10, pp. A53–A61, 2007.

[54] A. A. Govyadinov, V. A. Podolskiy, and M. A. Noginov, “Active metamaterials: sign of refractive index and gain-assisted dispersion management,” *Applied Physics Letters*, vol. 91, no. 19, Article ID 191103, 2007.

[55] A. K. Sarychev and G. Tartakovsky, “Magnetic plasmonic metamaterials in actively pumped host medium and plasmonic nanolaser,” *Physical Review B*, vol. 75, no. 8, Article ID 085436, 2007.

[56] O. Sydoruk, E. Shamonina, and L. Solymar, “Parametric amplification in coupled magnetoinductive waveguides,” *Journal of Physics D: Applied Physics*, vol. 40, no. 22, pp. 6879–6887, 2007.

[57] A. Bratkovsky, E. Ponizovskaya, S. Wang et al., “A metal-wire/quantum-dot composite metamaterial with negative ε and compensated optical loss,” *Applied Physics Letters*, vol. 93, no. 19, Article ID 193106, 2008.

[58] S. Chakrabarti, S. A. Ramakrishna, and H. Wanare, “Coherently controlling metamaterials,” *Optics Express*, vol. 16, no. 24, pp. 19504–19511, 2008.

[59] Z. Dong, H. Liu, T. Li et al., “Resonance amplification of left-handed transmission at optical frequencies by stimulated emission of radiation in active metamaterials,” *Optics Express*, vol. 16, no. 25, pp. 20974–20980, 2008.

[60] S. Chénais and S. Forget, “Recent advances in solid-state organic lasers,” *Polymer International*, vol. 61, no. 3, pp. 390–406, 2012.

[61] D. Bimberg, M. Grundmann, F. Heinrichsdorff et al., “Quantum dot lasers: breakthrough in optoelectronics,” *Thin Solid Films*, vol. 367, no. 1-2, pp. 235–249, 2000.

[62] V. I. Klimov, A. A. Mikhailovsky, S. Xu et al., “Optical gain and stimulated emission in nanocrystal quantum dots,” *Science*, vol. 290, no. 5490, pp. 314–317, 2000.

[63] I. Surez, H. Gordillo, R. Abargues, S. Albert, and J. Martínez-Pastor, “Photoluminescence waveguiding in CdSe and CdTe QDs-PMMA nanocomposite films,” *Nanotechnology*, vol. 22, no. 43, Article ID 435202, 2011.

[64] J. Grandidier, G. C. des Francs, S. Massenot et al., “Gain-assisted propagation in a plasmonic waveguide at telecom wavelength,” *Nano Letters*, vol. 9, no. 8, pp. 2935–2939, 2009.

[65] P. M. Bolger, W. Dickson, A. V. Krasavin et al., “Amplified spontaneous emission of surface plasmon polaritons and limitations on the increase of their propagation length,” *Optics Letters*, vol. 35, no. 8, pp. 1197–1199, 2010.

[66] S. Coffa, A. Polman, and R. N. Schwartz, *Rare Earth Doped Semiconductors II*, Materials Research Society, Pittsburgh, Pa, USA, 1996.

[67] J. Kalkman, C. Strohhöfer, B. Gralak, and A. Polman, "Surface plasmon polariton modified emission of erbium in a metallodielectric grating," *Applied Physics Letters*, vol. 83, no. 1, pp. 30–32, 2003.

[68] Y. Wang and Z. Zhou, "Strong enhancement of erbium ion emission by a metallic double grating," *Applied Physics Letters*, vol. 89, no. 25, Article ID 253122, 2006.

[69] S. John and T. Quang, "Spontaneous emission near the edge of a photonic band gap," *Physical Review A*, vol. 50, no. 2, pp. 1764–1769, 1994.

[70] W. L. Barnes, T. W. Preist, S. C. Kitson, and J. R. Sambles, "Physical origin of photonic energy gaps in the propagation of surface plasmons on gratings," *Physical Review B*, vol. 54, no. 9, pp. 6227–6244, 1996.

[71] S. C. Kitson, W. L. Barnes, and J. R. Sambles, "Surface-plasmon energy gaps and photoluminescence," *Physical Review B*, vol. 52, no. 15, pp. 11441–11445, 1995.

[72] Y. Wang and Z. Zhou, "Silicon optical amplifier based on surface-plasmon-polariton enhancement," *Applied Physics Letters*, vol. 91, no. 5, Article ID 053504, 2007.

[73] J. R. Lakowicz, "Radiative decay engineering 5: metal-enhanced fluorescence and plasmon emission," *Analytical Biochemistry*, vol. 337, no. 2, pp. 171–194, 2005.

[74] A. E. Christensen, C. Uhrenfeldt, B. Julsgaard, P. Balling, and A. N. Larsen, "Interaction between Au nanoparticles and Er^{3+} ions in a TiO_2 matrix: up-conversion of infrared light," *Energy Procedia*, vol. 10, pp. 111–116, 2011.

[75] E. Verhagen, L. Kuipers, and A. Polman, "Field enhancement in metallic subwavelength aperture arrays probed by erbium upconversion luminescence," *Optics Express*, vol. 17, no. 17, pp. 14586–14598, 2009.

[76] S. Gradečak, F. Qian, Y. Li, H. Park, and C. M. Lieber, "GaN nanowire lasers with low lasing thresholds," *Applied Physics Letters*, vol. 87, no. 17, Article ID 173111, 2005.

[77] M. A. Zimmler, J. Bao, F. Capasso, S. Müller, and C. Ronning, "Laser action in nanowires: observation of the transition from amplified spontaneous emission to laser oscillation," *Applied Physics Letters*, vol. 93, no. 5, Article ID 051101, 2008.

[78] R. Agarwal, C. J. Barrelet, and C. M. Lieber, "Lasing in single cadmium sulfide nanowire optical cavities," *Nano Letters*, vol. 5, no. 5, pp. 917–920, 2005.

[79] A. V. Maslov and C. Z. Ning, "Reflection of guided modes in a semiconductor nanowire laser," *Applied Physics Letters*, vol. 83, no. 6, pp. 1237–1239, 2003.

[80] P. J. Pauzauskie, D. J. Sirbuly, and P. Yang, "Semiconductor nanowire ring resonator laser," *Physical Review Letters*, vol. 96, no. 14, Article ID 143903, 2006.

[81] T. Zhang, G. Qian, Y.-Y. Wang et al., "Integrated optical gyroscope using active Long-range surface plasmon-polariton waveguide resonator," *Scientific Reports*, vol. 4, article 3855, 2014.

[82] M. T. Hill, M. Marell, E. S. P. Leong et al., "Lasing in metal-insulator-metal sub-wavelength plasmonic waveguides," *Optics Express*, vol. 17, no. 13, pp. 11107–11112, 2009.

[83] R. Ma, R. F. Oulton, V. J. Sorger, G. Bartal, and X. Zhang, "Room-temperature sub-diffraction-limited plasmon laser by total internal reflection," *Nature Materials*, vol. 10, no. 2, pp. 110–113, 2011.

[84] H. Raether, "Surface plasmons on gratings," in *Surface Plasmons on Smooth and Rough Surfaces and on Gratings*, pp. 91–116, 1988.

[85] D. J. Bergman and M. I. Stockman, "Surface plasmon amplification by stimulated emission of radiation: quantum generation of coherent surface plasmons in nanosystems," *Physical Review Letters*, vol. 90, no. 2, Article ID 027402, 2003.

[86] M. A. Noginov, G. Zhu, A. M. Belgrave et al., "Demonstration of a spaser-based nanolaser," *Nature*, vol. 460, no. 7259, pp. 1110–1112, 2009.

[87] V. J. Sorger and X. Zhang, "Spotlight on plasmon lasers," *Science*, vol. 333, no. 6043, pp. 709–710, 2011.

[88] R. A. Flynn, C. S. Kim, I. Vurgaftman et al., "A room-temperature semiconductor spaser operating near 1.5 μm," *Optics Express*, vol. 19, no. 9, pp. 8954–8961, 2011.

[89] J. K. Kitur, V. A. Podolskiy, and M. A. Noginov, "Stimulated emission of surface plasmon polaritons in a microcylinder cavity," *Physical Review Letters*, vol. 106, no. 18, Article ID 183903, 2011.

[90] M. Walter, J. Walowski, V. Zbarsky et al., "Seebeck effect in magnetic tunnel junctions," *Nature Materials*, vol. 10, no. 10, pp. 742–746, 2011.

[91] M. J. H. Marell, B. Smalbrugge, E. J. Geluk et al., "Plasmonic distributed feedback lasers at telecommunications wavelengths," *Optics Express*, vol. 19, no. 16, pp. 15109–15118, 2011.

[92] K. Ding, Z. Liu, L. Yin et al., "Electrical injection, continuous wave operation of subwavelength-metallic- cavity lasers at 260 K," *Applied Physics Letters*, vol. 98, no. 23, Article ID 231108, 2011.

[93] E. Cubukcu, E. A. Kort, K. B. Crozier, and F. Capasso, "Plasmonic laser antenna," *Applied Physics Letters*, vol. 89, no. 9, Article ID 093120, 2006.

[94] N. Yu, J. Fan, Q. J. Wang et al., "Small-divergence semiconductor lasers by plasmonic collimation," *Nature Photonics*, vol. 2, no. 9, pp. 564–570, 2008.

[95] J. A. Rogers, M. Meier, A. Dodabalapur, E. J. Laskowski, and M. A. Cappuzzo, "Distributed feedback ridge waveguide lasers fabricated by nanoscale printing and molding on nonplanar substrates," *Applied Physics Letters*, vol. 74, no. 22, pp. 3257–3259, 1999.

[96] H. Ma, A. K.-Y. Jen, and L. R. Dalton, "Polymer-based optical waveguides materials, processing, and devices," *Advanced Materials*, vol. 14, no. 19, pp. 1339–1365, 2002.

[97] M. T. Hill, Y. Oei, B. Smalbrugge et al., "Lasing in metallic-coated nanocavities," *Nature Photonics*, vol. 1, no. 10, pp. 589–594, 2007.

[98] D. Amarasinghe, A. Ruseckas, A. E. Vasdekis, M. Goossens, G. A. Turnbull, and I. D. W. Samuel, "Broadband solid state optical amplifier based on a semiconducting polymer," *Applied Physics Letters*, vol. 89, no. 20, Article ID 201119, 2006.

[99] D. Amarasinghe, A. Ruseckas, A. E. Vasdekis, G. A. Turnbull, and I. D. W. Samuel, "Amplification of optical pulse sequences at a high repetition rate in a polymer slab waveguide," *Applied Physics Letters*, vol. 91, no. 1, Article ID 011105, 2007.

[100] S. Kéna-Cohen, P. N. Stavrinou, D. D. C. Bradley, and S. A. Maier, "Confined surface plasmon-polariton amplifiers," *Nano Letters*, vol. 13, no. 3, pp. 1323–1329, 2013.

[101] I. de Leon and P. Berini, "Spontaneous emission in long-range surface plasmon-polariton amplifiers," *Physical Review B*, vol. 83, no. 8, Article ID 081414, 2011.

[102] I. de Leon and P. Berini, "Theory of noise in high-gain surface plasmon-polariton amplifiers incorporating dipolar gain media," *Optics Express*, vol. 19, no. 21, pp. 20506–20517, 2011.

[103] I. De Leon and P. Berini, “Gain and noise in long-range surface plasmon-polariton amplifiers,” in *CLEO: Applications and Technology*, p. JTuI30, Optical Society of America, 2011.

[104] P. Berini, “Plasmon-polariton modes guided by a metal film of finite width bounded by different dielectrics,” *Optics Express*, vol. 7, no. 10, pp. 329–335, 2000.

[105] R. Charbonneau, C. Scales, I. Breukelaar et al., “Passive integrated optics elements based on long-range surface plasmon polaritons,” *Journal of Lightwave Technology*, vol. 24, no. 1, pp. 477–494, 2006.

[106] A. Boltasseva and S. I. Bozhevolnyi, “Directional couplers using long-range surface plasmon polariton waveguides,” *IEEE Journal on Selected Topics in Quantum Electronics*, vol. 12, no. 6, pp. 1233–1241, 2006.

[107] J. T. Kim, S. Park, J. J. Ju, S. K. Park, M. Kim, and M. Lee, “Low-loss polymer-based long-range surface plasmon-polariton waveguide,” *IEEE Photonics Technology Letters*, vol. 19, no. 18, pp. 1374–1376, 2007.

[108] T. Nikolajsen, K. Leosson, and S. I. Bozhevolnyi, “Surface plasmon polariton based modulators and switches operating at telecom wavelengths,” *Applied Physics Letters*, vol. 85, no. 24, pp. 5833–5835, 2004.

[109] G. Gagnon, N. Lahoud, G. A. Mattiussi, and P. Berini, “Thermally activated variable attenuation of long-range surface plasmon-polariton waves,” *Journal of Lightwave Technology*, vol. 24, no. 11, pp. 4391–4402, 2006.